# Polyethylenimine-mediated synthetic insertion of gold nanoparticles into mesoporous silica nanoparticles for drug loading and biocatalysis

P C Pandey<sup>a\*</sup>, Govind Pandey<sup>b</sup> and Roger J. Narayan<sup>c</sup>

<sup>a</sup>Department of Chemistry, Indian Institute of Technogy (BHU), Varanasi-221005, India pcpandey.apc@iitbhu.ac.in

<sup>b</sup>BRD Medical College, Gorakhpur-273013, India

<sup>c</sup>Joint Department of Biomedical Engineering, University of North Carolina and North Carolina State University, Raleigh, NC, USA;

roger\_narayan@unc.edu

#### **ABSTRACT**

Mesoporous silica nanoparticles (MSNPs) have been used as an efficient and safe carrier for drug delivery and biocatalysis. The surface modification of MSNPs using suitable reagents may provide a robust framework in which two or more components can be incorporated to give multifunctional capabilities (e.g., synthesis of noble metal nanoparticles within a mesoporous architecture along with loading of a bioactive molecule). In this study, the authors reported on a new synthetic route for the synthesis of gold nanoparticles (AuNPs) within (a) unmodified MSNPs and (b) 3-trihydroxysilvlpropyl methylphosphonate-modified MSNPs. A cationic polymer, polyethylenimine (PEI), and formaldehyde were used to mediate synthetic incorporation of AuNPs within MSNPs. The AuNPs incorporated within the mesoporous matrix were characterized by transmission electron microscopy, energy dispersive Xray analysis, and high-resolution scanning electron microscopy. PEI in the presence of formaldehyde enabled synthetic incorporation of AuNPs in both unmodified and modified MSNPs. The use of unmodified MSNPs was associated with an increase in the polycrystalline structure of the AuNPs within the MSNPs. The AuNPs within modified MSNPs showed better catalytic activity than those within unmodified MSNPs. MSNPs with an average size of 200 nm and with a pore size of 4-6 nm were used for synthetic insertion of AuNPs. It was found that the PEI coating enabled AuNP synthesis within the mesopores in the presence of formaldehyde or tetrahydrofuran hydroperoxide at a temperature between 10-25 °C or at 60°C in the absence of organic reducing agents. The asmade AuNP-inserted MSNPs exhibited enhanced catalytic activity. For example, these materials enabled rapid catalytic oxidation of the o-dianisidine substrate to produce a blue colored solution in proportion to the amount of H<sub>2</sub>O<sub>2</sub> generated as a function of glucose oxidase-catalyzed oxidation of glucose; a linear concentration range from 80 to 800 µM and a detection limit as low as 80 µM were observed. The mesoscale pores of the as developed AuNP-inserted MSNPs were also used to entrap the hydrophobic drug paclitaxel. The results of this study indicate the potential use of the AuNP-inserted MSNPs in biocatalysis and drug delivery.

## **KEYWORDS**

Mesoporous silica, silver nanoparticles, biocatalysis, drug delivery

#### INTRODUCTION

Porous materials have technological significance since these structures may interact with active molecules and metal nanoparticles. One important category is mesoporous silica (MPS) and mesoporous silica nanoparticles (MSNP); these materials were first described by Kuroda et al. in 1990 and have received attention for adsorption/separation, catalytic and sensing applications. The preparation of MSNPs involves the use of ion-surfactants (e.g., alkyltrimethylammonium halides) to form a lyotropic liquid-crystalline phase that enables self-assembly of silica frameworks via condensation of silica oligomers. These materials can be tailored via organic or magnetic functionalization to enhance their ability to interact with other species. Functionalization of MSNP with 3-trihydroxysilylpropyl methylphosphonate enabled selective coating of a cationic polymer, polyethylenimine (PEI), providing capabilities for drug loading and delivery. This study is focused on surface functionalization of MSNPs with 3-trihydroxysilylpropyl methylphosphonate and PEI and the use of these materials for biocatalysis and drug loading.

Gold nanoparticles that are functionalized with suitable agents allow for both selective imaging and photothermal killing of cancer cells.<sup>7-9</sup> The size of the mesoporous material plays an important role for in vivo biomedical applications. The mesoporous architecture can be utilized for selective drug loading<sup>6</sup>; synthetic insertion of gold nanoparticles into MSNPs may provide useful biomedical functionality. Attempts have been made to incorporate gold nanoparticles in mesoporous MCM-41/MCM-48 through including a suspension of AuNPs in the synthesis of MCM-41/MCM-48.<sup>10</sup> Nakanishi et al. recently reported on the synthesis of AuNPs in a mesoporous silica sheet. 11 This study demonstrated that a suspension of amino-functionalized silica material in an ethanolic solution of gold salt that was sonicated for 1 h introduced the gold precursor into the mesopores. The resulting materials were collected via centrifugation, vacuum dried at room temperature for 6 h, and calcined in a muffle furnace at 550° C with a controlled heating rate. Due to size of MCM-41/MCM-48 and mesoporous silica sheet, AuNPs that are inserted into mesoporous MCM-41/MCM-48 and mesoporous silica sheet are not suitable for in vivo biomedical applications; on the other hand, the insertion of AuNPs in the mesoporous architecture of MSNPs under ambient conditions may allow for loading of a suitable drug. Recently, the use of mesoporous silica-encapsulated gold nanoparticles as artificial enzymes for self-activated cascade catalysis was reported by Lin et al. 19 These authors reduced gold cations in a suspension of gold cation-containing 3-aminopropyltrimethoxysilane-modified MSNPs using sodium borohydride (NaBH<sub>4</sub>). This process resulted in a decrease in the crystallinity of the MSNPs and restricted the loading of targeted drugs and gold nanoparticles within the mesopores. In addition to that, the use of sodium borohydride is not a reasonable regent for in situ generation of biomaterials. Accordingly, there is a need for charged MSNP nanoparticles that facilitate drug loading, provide sites for synthetic insertion of gold nanoparticles, and enable simultaneous loading of targeted drugs for delivery.

We have recently demonstrated the role of a cationic polymer, PEI, which not only allows the rapid reduction of gold cations into gold nanoparticles in the presence of formaldehyde but also allows the formation of cationic coating for drug loading. The use of AuNPs for medical applications has been previously demonstrated. 13-20 It should be noted that AuNPs in a homogeneous suspension have limited capabilities for targeted drug loading. A robust framework in which two or more components can be incorporated to

provide multifunctional capabilities is preferable. AuNPs may be loaded onto nontoxic MSNPs for therapeutic applications. 6 In this study, synthetic insertion of AuNPs in MSNPs for drug loading was explored. The use of PEI introduces a cationic coating, which generates a positive charge on MSNP and facilitates electrostatic interaction of a suitable drug within the mesoporous architecture. A synthetic approach reported earlier<sup>12</sup> may allow for PEI-mediated synthetic insertion of AuNPs with controlled nanogeometry in MSNPs, providing a novel platform for drug loading and efficient bio-catalytic activity. The modification of MSNPs with PEI facilitates synthetic insertion of AuNPs in the mesoporous architecture of MSNPs. We intend to enhance the selective binding of PEI through surface modification of MSNPs using the reagent 3-trihydroxysilylpropyl methylphosphonate, which has already been shown to act as an effective surface modifier for selective drug loading and drug delivery. 6. Control over the size of MSNPs is an important requirement for facilitating in vivo biomedical applications of AuNP-inserted MSNPs; MSNPs with an average size of 200 nm and a mesoporous architecture of 4-6 nm were used for synthetic insertion of AuNPs in the present study. The concentration of PEI influences the synthetic incorporation of AuNPs within the mesoporous architecture of the silica nanoparticles. Data was obtained involving use of two concentrations of PEI and a single concentration of formaldehyde for synthetic insertion of AuNPs within unmodified MSNPs and 3-trihydroxysilylpropyl methylphosphonate-modified MSNPs. The AuNPs inserted MSNPs were evaluated using photographic imaging, transmission electron microscopy (TEM), energy dispersive X-ray analysis (EDAX), and high resolution scanning electron microscopy (HR SEM). Applications of the as-made material in catalysis and loading of paclitaxel were evaluated. As reported earlier, AuNP-incorporated MSNPs were shown to possess enhanced catalytic activity for glutathione (GSH) and peroxidase mimetic activity for glucose sensing. 12, 20

# II. EXPERIMENTAL

#### **Materials**

Tetraethylorthosilicate, 3-(trihydroxysilyl) propyl methylphosphonate (42%), and polyethylenimine (50 wt. % in H<sub>2</sub>O, average M<sub>n</sub> 1200, 60000, 25000) were obtained from Sigma-Aldrich. Tetrachloroauric acid hydrate was purchased from HiMedia. Acetaldehyde, acetone, and tert- butyl methyl ketone were obtained from Merck (India). All other chemicals employed were of analytical grade. Aqueous solutions were prepared using doubly distilled-deionized water. Unless mentioned otherwise, all of the experiments were performed at room temperature (25°C). TEM) images were recorded using a Morgagni 268D (FEI Electron Optics) instrument that was operated at 200 kV.

# Synthesis of mesoporous silica nanoparticles (MSNPs)

Synthesis of MSNPs was conducted by mixing tetraethylorthosilicate (TEOS) with cetyltrimethylammonium bromide (CTAB) in a basic aqueous solution (pH 11). In a round-bottom flask, 50 mg of CTAB was dissolved in a solution containing 20 ml of

distilled water and 150 µl of sodium hydroxide (2 M). The solution was heated to 82 °C with stirring followed by drop wise addition of 240 µl of TEOS into the reaction at 82°C. The reaction mixture was subsequently cooled to room temperature and the materials were washed with methanol through centrifugation. The surfactants were removed from the pores by refluxing the particles in a mixture of methanol and hydrochloric acid for 24 h. The MSNPs were then centrifuged and washed with methanol. Some of the asmade MSNPs were used for PEI functionalization.

### Synthetic insertion of gold nanoparticles with MSNPs

Previous studies demonstrated the role of PEI in reducing gold cations to gold nanoparticles in the presence of formaldehyde. <sup>12,21,22</sup> In this study, PEI is used during synthetic incorporation of gold nanoparticles in MSNPs to create a cationic charge around the MSNPs for drug loading. In addition, surface modification of MSNPs with 3-trihydroxysilylpropyl methyl phosphonate may enable selective coating of PEI on MSNPs and as such may further enhance the loading of hydrophobic cancer drug paclitaxel. Surface modification using 3-trihydroxysilylpropyl methyl phosphonate and PEI play central roles in the synthetic incorporation of gold nanoparticles within MSNPs.

# i) Surface modification of MSNP by 3-trihydroxysilylpropyl methyl phosphonate

50 mg of MSNP was suspended in 1 ml of distilled water containing 5% w/v 3-trihydroxysilylpropyl methyl phosphonate and stirred for 2 hours at 40°C. The modified MSNPs were cooled and collected by centrifugation followed by careful washing with water and finally with ethanol. The 3-trihydroxysilylpropyl methyl phosphonate functionalized MSNPs were dried at 60°C overnight.

# ii) Polyethylenimine mediated synthetic insertion of AuNPs into mesoporous architecture of MSNPs

Both unmodified and 3-trihydroxysilylpropyl methyl phosphonate modified MSNPs were used for PEI-mediated synthetic insertion of AuNPs. Two stock solutions of PEI in lower aliphatic alcohol (8 mg/ml and 5 mg/ml) were chosen for modification of the MSNPs. 200 µl of PEI in 9% w/v ethanolic solution was added to 10 mg of unmodified/modified MSNPs; continuous stirring for 1-2 hours at 25°C was performed on this solution. The PEI-treated MSNPs were collected by centrifugation and washed several times to ensure removal of unbound PEI. 50 µl formaldehyde solution in ethanol (40 % w/v) was added to the 200 µl ethanolic suspension of PEI treated MSNPs; this solution was constantly stirred for 2 hours at 25°C. The as-made AuNPs within unmodified or modified MSNPs were collected by centrifugation and were washed with lower aliphatic alcohol/ethanol several times to ensure complete removal of unbound AuNPs. The washed AuNPs may be suspended in the desired aqueous or ethanolic medium or may be dried at 60°C overnight to obtain AuNP-inserted MSNP powder.

#### iii) Characterization of AuNP-inserted MSNPs

The as-made AuNP-incorporated MSNPs were evaluated using photographs, transmission electron microscopy, EDAX, and HR SEM. The size of nanoparticles and the overall distribution in suspension were determined by transmission electron microscopy at different magnifications. The crystallinity of the as-made AuNPs was determined from the selected area electron diffraction pattern.

### Peroxidase Mimetic Activity of AuNP-incorporated MSNPs

The peroxidase-like activity of the as-synthesized AuNP-incorporated MSNPs was determined spectrophotometrically by measuring the formation of the oxidized reaction product of o-dianisidine, which has an absorption maximum at 430 nm, using a Hitachi U-2900 spectrophotometer. The o-dianisidine oxidation activity was measured in 2 mL phosphate buffer (0.1 M, pH 7.0) in the presence of 2 mg of the MSNPs and 60 µM o-dianisidine at 25°C. H<sub>2</sub>O<sub>2</sub>(1 mM) was added to start the reaction.

Glucose sensing based on peroxidase mimetic activity of the AuNP-incorporated MSNPs has also been examined using the previously described approach that involves the formation of hydrogen peroxide through glucose oxidase-catalyzed oxidation of glucose. The glucose oxidase (100 U) was dissolved in phosphate buffer followed by the addition of AuNP-incorporated MSNPs (2 mg) followed by the addition of o-dianisidine (2 mM). Known concentrations of glucose were added under stirring and allowed the catalyzed reaction to proceed for 45 minutes. The formation of a coloured product of oxidized o-dianisidine was monitored spectrophotometrically at 430 nm. Several concentrations of glucose were used to construct the calibration curve for glucose analysis.

#### **GSH** sensing based on competitive binding

The GSH samples were detected as described earlier  $^{12}$  according to the following steps: 40  $\mu$ L of 3.2 M H<sub>2</sub>O<sub>2</sub>, 25  $\mu$ l of several concentrations of GSH, 70  $\mu$ L of 10 mM o-dianisidine, and 2 mg of AuNP-incorporated MSNPs were added to 800  $\mu$ L of water. After incubating for 25 minutes, the UV-Vis spectrum of the reaction product was monitored for each GSH system using a spectrophotometer (Hitachi U-2900) in wavelength scan mode. The absorbance change at 430 nm was used for detecting the concentration of GSH. The final concentration of GSH in the system varied between 10 nM and 100  $\mu$ M

## Paclitaxel loading in AuNP-incorporated MSNPs

The AuNP-inserted silica nanoparticles were loaded with paclitaxel by incubating the nanoparticles in a solution containing a high concentration of the drug in DMSO. 10 mg of the nanoparticles was incubated for 6 h in a solution containing 1 mg of paclitaxel in 0.25 mL of DMSO. After the drug-laden nanoparticles were removed from the suspension by centrifugation, the supernatant was completely removed; the product was dried under vacuum. The drug-laden nanoparticles were washed and sonicated with PBS. In order to determine the amount of paclitaxel that partitioned to the MSNPs, the aqueous particle suspension was incubated for 6 h at 4 °C before centrifugation. Methanol was used to release paclitaxel from the MSNPs and obtain the loading capacity. The drug-laden

MSNP pellet was resuspended and sonicated in methanol three times. The supernatants were combined to evaluate drug release; UV absorption measurements at a wavelength of 230 nm were used to obtain drug release data.

The contribution of PEI during drug loading ability was also evaluated. The AuNP-inserted MSNPs were made by modifying the surface of phosphonate-coated MSNPs in the presence of several concentrations of PEI between 4 mg/ml to 10 mg/ml. After careful washing and drying, the as-made AuNP-inserted MSNPs were used in drug loading studies.

#### RESULTS AND DISCUSSION

# **Synthesis of MSNPs**

TEOS in the presence of the templating surfactant CTAB in basic aqueous medium allows for the controlled conversion of silica precursors into MSNPs. The size of the MSNPs is a function of the dynamics of TEOS hydrolysis in basic medium; the pore size is a function of the templating surfactant. Under the present experimental conditions, MSNPs with an average particle size on the order of 200 nm were isolated. As shown in the TEM images, the size of mesopores after surfactant removal was found to be 4-6 nm.

# Synthetic insertion of AuNPs in MSNPs

Although findings reported earlier<sup>12</sup> demonstrated rapid conversion of gold cations into AuNPs, the synthesis of AuNPs within a mesoporous architecture might not lead to effective insertion of AuNPs within a mesoporous architecture due to variation in the dynamics of organic moiety-mediated reduction of gold cations within a heterogeneous matrix. Accordingly, we intend to overcome this limitation following two-step process; (1) conditioning of PEI-functionalized MSNPs in an ethanolic solution of gold cations under stirring and (2) functionalization of MSNPs by 3-trihydroxysilylpropyl methyl phosphonate. The concentration of PEI may play a crucial role during synthetic incorporation of AuNPs in MSNPs; as such, understanding the effect of PEI concentration on the synthetic insertion of AuNPs within MSNPs is also desirable. Step 1 ensures the availability of gold cations within the mesoporous architecture and step 2 enables selective binding of PEI, which may easily facilitate the conversion of gold cations into AuNPs within heterogeneous matrix.

The earlier findings on AuNP synthesis demonstrate that PEI enables rapid (within two minutes) conversion of gold cations into AuNPs in the presence of formaldehyde. <sup>12</sup> It was found that PEI plays a central role during nanoparticle synthesis. Both unmodified MSNP were treated with desired concentrations of PEI, followed by careful washing to ensure complete removal of unbound PEI. The initial findings demonstrated that both lower and much higher concentrations of PEI are not suitable for synthetic insertion of AuNPs in MSNPs since the PEI concentration also controls the nanoscale geometry of the in situ generated AuNPs. <sup>12</sup> The use of higher concentrations of PEI (> 15 mg/ml) resulted in agglomeration of surface attached AuNPs. Lower concentrations of PEI (< 3 mg/ml) did not allow the conversion of gold cations into AuNPs. Accordingly, the synthetic insertion of AuNPs in MSNPs was investigated at two optimal concentrations of PEI: 5 mg/ml and 8 mg/ml.

The photographs of MSNPs and AuNP-inserted MSNPs are shown in Figure 1a; Fig.1b shows the suspension of MSNPs and AuNP-inserted MSNPs in an ethanolic medium. Both MSNPs and AuNP-inserted MSNPs were well dispersed in either aqueous or ethanolic media (Fig.1).

## Characterization of AuNP-inserted MSNPs

The AuNPs inserted in both unmodified and modified MSNPs at two concentration of PEI (5 mg/ml and 8 mg/ml) were characterized using TEM. Figure 2 shows TEM images of AuNPs inserted in unmodified MSNPs at two concentrations of PEI (L=5mg/ml and H=8mg/ml). The average size of the AuNPs was found to be 8.33 nm and 8.11 at the lower and higher concentrations of PEI, respectively. It is also noteworthy that an increase in PEI concentration allows for a significant increase in the number of AuNPs inserted within the MSNPs (Figure 2). As shown in Figure 3, similar results were recorded for modified MSNPs. The average size of gold nanoparticles was found to be 6.95 and 5.98 nm at the lower and higher concentrations of PEI, respectively. The selected area electron diffraction pattern (SAED) and EADX of AuNPs inserted in unmodified and modified MSNPs are shown in Figure 4 and Figure 5, respectively. The findings indicated that there is more polycrystallinity in the AuNPs that are inserted in unmodified MSNPs. A few results involving PEI- and formaldehyde-mediated synthetic insertion of AuNPs are summarized as follows: (i) an increase in PEI concentration resulted in better insertion of AuNPs into the mesoporous architecture, (ii) a larger number of AuNPs were located within the mesoporous architecture as the PEI concentration was increased, (iii) modification of MSNPs by 3-trihydroxysilylpropyl methyl phosphonate facilitated better synthetic insertion of AuNPs into the mesoporous architecture, and (iv) a wide size distribution of AuNP size was found on unmodified MSNPs whereas a narrow size distribution of AuNP size was found on modified MSNPs. The findings indicate that the trihydroxysilylpropyl methyl phosphonate coating introduced selectivity that allowed for better binding of PEI on the MSNP surface, which facilitated better synthetic insertion of AuNPs within the mesoporous architecture of the MSNPs. The TEM images (Figure 2-3) indicate that the AuNPs are strongly attached to the porous MSNPs. The average size of the AuNPs linked to the MSNPs was found to be 8-9 nm with unmodified MSNPs and 5-6 nm for modified MSNPs. HR SEM data from the unmodified and modified MSNPs is shown in Figure 6 and Figure 7 and confirms previous results involving the synthetic incorporation of AuNPs within mesoporous silica nanoparticles. The MSNPs made in this investigation have an average size of 200 nm and a pore size of 4-6 nm. The size of the in situ generated AuNPs plays an important role during synthetic incorporation into the mesoporous architecture. Accordingly, the insertion of AuNPs within MSNPs architecture requires control over the porosity and size of the MSNPs along with precise control over the size of the in situ generated gold nanoparticles. The reproducibility of process for modification of 200 nm size MSNPs by PEI times has been repeated many times. Each attempt involving nanoparticle synthesis within MSNPs through the current process yielded reproducible results.

# Peroxidase mimetic ability of AuNP-inserted MSNPS.

AuNPs have been previously evaluated for use as a peroxidase mimetic agent.<sup>20</sup> Use of PEI-stabilized AuNPs as a peroxidase mimetic for homogeneous catalysis is shown in Figure 8. Accordingly, we examined the H<sub>2</sub>O<sub>2</sub>-mediated oxidation of o-dianisidine in the presence of as-made AuNP-inserted MSNPs. The time-dependent kinetic measurement of AuNP-mediated catalytic oxidation of colorless reduced o-dianisidine to colored oxidized o-dianisidine is shown in Figure 9. Since the relative concentration of AuNP-inserted MSNPs with surface functionalization is higher, the catalytic activity is better for AuNP-inserted modified MSNPs (Figure 9).

Efforts were undertaken to understand the catalytic activity of AuNP-inserted MSNPs and MSNPs in absence of AuNPs. It should be noted here that AuNP-inserted MSNPs made with a high concentration of PEI (i.e. 8 mg/ml) were used for this evaluation. The results shown in Figure 9b clearly demonstrate the efficient catalytic activity of AuNPs as a peroxidase mimetic as reported earlier. <sup>20</sup> The results confirm that modified MSNPs show better catalytic activity for practical applications as compared with unmodified AuNP-inserted MSNPs and MSNP without AuNPs (Figure 9b).

Glucose oxidase-catalyzed reactions were used to evaluate the peroxidase mimetic activity of the materials. The AuNPs inserted in modified MSNPs were incubated with 100 U of glucose oxidase with desired concentrations of glucose and incubated for 45 minutes. The as-generated hydrogen peroxide was monitored using o-dianisiding as chromogen. The formation of a color reaction product as a function of glucose concentration is shown in Figure 9c. The results as shown in Figure 9c justify the catalytic potential of as made AuNP-inserted MSNPs for glucose biosensing with a lowest detection limit of 80 µM glucose (Figure 9d).

# Glutathione sensing based on competitive binding

The results shown in Figures 10-11 justified the excellent catalytic activity of AuNP-inserted MSNPs as a peroxidase mimetic. In addition, it was shown that there is competitive interaction of  $H_2O_2$  between GSH and o-dianisidine as shown below:

$$H_2O_2 + 2 GSH \rightarrow H_2O + GSSG...$$
 (2)

Based on the competitive reaction shown in equations (1) and (2), an increase in GSH concentration causes less conversion of reduced o-dianisidine to a colored reaction product (Figure 10a). Quantitative analysis of GSH sensing was evaluated using UV-Vis spectroscopy; formation of the colored reaction product o-dianisidine in the presence of GSH was recorded in Figure 10b. *Ten* standard samples of GSH were analyzed based on the current approach and matched to original concentrations between 10 nm and 400  $\mu$ M (Figure 10b). As shown in Figure 10c, the analytical data yielded an excellent detection limit; a lowest detection of 22 +3 nM

was recorded. The reported method of gold nanoparticle synthesis is more efficient and reproducible for yielding a desirable AuNP nanogeometry based on an appropriate choice of PEI, gold cation, and organic reducing agent concentrations (Figure 10d).

The relative catalytic ability of (i) the AuNP homogeneous suspension, (ii) AuNP-inserted unmodified MSNPs, and (iii) AuNP-inserted modified MSNPs as a peroxidase mimetic was assessed via GSH detection. The catalytic activity of these nanocatalysts is shown in Figure 11. The finding indicates that the AuNP suspension is relatively more catalytic than the AuNP-inserted MSNPs under similar experimental conditions. This result may be due to the relatively high surface area of AuNPs for specific interactions.

# Paclitaxel loading in AuNP-inserted MSNPs

One of the potential applications of the nanomaterial involves use in drug loading. Accordingly, paclitaxel loading in AuNP-incorporated MSNP was studied. In order to determine the amount of paclitaxel that was stored in the MSNPs (i.e., the loading capacity), methanol was used to release paclitaxel from MSNPs. The drug-laden MSNP was resuspended and sonicated in methanol on three occasions; UV absorption at 230 nm was used to measure the release of the drug in the combined supernatants. It was observed that the concentration of PEI used during modification plays an important role in the drug storing functionality of AuNP-inserted MSNPs. The relative percent loading of the AuNP-inserted MSNPs is shown in Figure 11a. The findings shown in Figure 11a revealed that the amount of loaded paclitaxel was a function of the PEI concentration. Accordingly, the effect of PEI concentration was investigated to evaluate the drug loading functionality of AuNP-inserted MSNPs. The results as shown in Figure 11b justify the effect of PEI on drug loading functionality of the nanoparticles. 1 mg/ml of AuNP encapsulated MSNPs made with 10 mg/ml PEI stored 18 µM of paclitaxel. The drug loading functionality of surface functionalized MSNPs was found to be better than that of unmodified MSNPs (Figure 11a) due to increase in selectivity provided by PEI-mediated binding of the drug.

Finally, it is important to review the contribution of the PEI coating to drug loading and drug delivery. The presence of a positive charge on the MSNP may increase the delivery of negatively charged nucleic acids to cells. Since PEI is a cationic polymer, the PEI coating creates a positively charged MSNP that can be used to increase the delivery of nucleic acid to cell<sup>12</sup> and has been described as an alternative to traditional viral vectors. The concentrations of two surface modifiers, 3-trihydroxysilylpropyl methylphosphonate and PEI, may be altered as appropriate may facilitate the loading of the hydrophobic cancer drug paclitaxel within mesoporous architecture. The initial findings demonstrated an enhanced loading ability of AuNP-inserted MSNPs as the PEI concentration was increased. This study demonstrates both drug loading and biocatalysis functionalities of the AuNP-inserted MSNPs. The release of hydrophobic drugs from the MSNPs in water is slow and is currently under detailed investigation.

# CONCLUSIONS

The present article demonstrates a novel approach for synthetic insertion of gold nanoparticles into mesoporous silica nanoparticles. Polyethylenimine-mediated synthetic insertion of AuNPs into MSNPs with an average size on the order of 200 nm and with pore size of 4-6 nm in the presence of formaldehyde was demonstrated. EADX and TEM analysis indicated that surface functionalization of MSNPs with 3-trihydroxysilylpropyl methyl phosphonate facilitated synthetic insertion of AuNPs into MSNPs. The AuNP-inserted MSNPs showed biocatalytic activity and served as a robust framework for paclitaxel loading, indicating potential use of these materials for multiple technological applications.

# **ACKNOWLEDGEMENTS**

The authors would like to acknowledge support from the University Grants Commission (UGC) for a one time grant.

### REFERENCES

- <sup>1</sup> T, Yanagisawa, T. Shimizu, K. Kuroda, and C. Kato, Bull Chem Soc Jpn, 63, 988(1990).
- <sup>2</sup> I. Snagaki, Y. Fukushima, and K. Kuroda, *J Chem Soc Chem Commun*, 8, 680 (1993).
- <sup>3</sup> F. Hoffmann, M. Cornelius, J. Morell and M. Froeba, *Angew Chem Int Ed*, 45, 3216 (2006).
- <sup>4</sup> A. P. Wight and M. E. Davis, *Chem Rev*, 102, 3589 (2002).
- <sup>5</sup> P. Yang, S. Gai, and J. Lin, *J Chem Soc Rev*, 41, 3679 (2012).
- <sup>6</sup>T. Xia, M. Kovochich, M. Liong, H. Meng, S. Kabehie, S. George, J. I. Zink and A.E. Nel, ACS Nano 3, 3273(2009).
- <sup>7</sup> X. Huang, I. H. El-Sayed. W. Qian and M. A. El-Sayed, *J Am Chem Soc*, 128, 2115 (2006).
- <sup>8</sup> J. Chen, D. Wang, J. Xi, L. Au, A. Siekkinen, A. Warsen, Z. Y. Li, H. Zhang, Y. Xia and X. Li, Nano Lett, 7, 1318 (2007).
- <sup>9</sup> A. M. Gobin , M. H. Lee, N. J. Halas , W. D. James, R. A. Drezek and J. L. West, *Nano Lett*, 7, 1929 (2007).
- <sup>10</sup> Z. Konya, V. F. Puntes, I. Kiricsi, J. Zhu, J. W. Ager, M. K. Ko, H. Frei, P. Alivisatos and G. A. Somorjai, *Chem Mater*, *15*, 1242 (2003).
- <sup>11</sup> K. Nakanishi, M. Tomita, Y. Masuda, and K. Kato, New J Chem, 39, 4070 (2015).
- <sup>12</sup> P. C. Pandey, G. Pandey, and R. J. Narayan. J Biomed Mater Res Part B, (2015) DOI: 10.1002/jbm.b.33647.
- <sup>13</sup> R. Cao-Milan, and L. M. Liz-Marzan, Exp Opin Drug Deliv, 11, 741 (2014).
- <sup>14</sup> Y. K. Mishra, S. Mohapatra, D. K. Avasthi, D. Kabiraj, N. P. Lalla, J. C. Pivin, H. Sharma, R. Kar, and N. Singh, *Nanotechnol*, 18, 345606 (2007).
- <sup>15</sup> P. K. Jain, K. S. Lee, I. H. El-Sayed, and M. A. El-Sayed, *J. Phys. Chem. B*, 110, 7238 (2006).
- <sup>16</sup> X. Huang, P. K. Jain, I. H. El-Sayed, and M. A. El-Sayed, *Nanomed*, 2, 681 (2007).
- <sup>17</sup> E. Aznar, M. Oroval, L. Pascual, J. R. Murguía, R. Martínez-Máñez, and F. Sancenón, *Chem Rev.*, 116 (2), 561 (2016).
- <sup>18</sup> F. Sancenón, L. Pascual, M. Oroval, E. Aznar, and R. Martínez-Máñez, *ChemistryOpen*, 4, 418 (2015). DOI:
- 10.1002/open.201500053
- <sup>19</sup> Y. Lin, Z. Li, Z. Chen, J. Ren and X. Ou, *Biomaterials*, 34, 2600(2013).
- <sup>20</sup> S. Cho, H. Y. Shin and M. I. I. Kim, *Biointerface* 12(1), 01A401-1(2017)
- <sup>21</sup> P. C. Pandey and G. Pandey, *Indian Patent* 4043/DEL/2014.
- <sup>22</sup> P. C. Pandey and G. Pandey, *Indian Patent* 201611052267.

#### FIGURE CAPTIONS

- Figure 1 (A) Image of MSNP and AuNP-inserted MSNP powders. b) Image of MSNP and AuNP-inserted MSNP suspension in ethanol.
- Figure 2. TEM images of AuNP-inserted unmodified MSNPs that were made using two concentrations of PEI (L=5 mg/ml and H=8 mg/ml).
- Figure 3. TEM images of AuNP-inserted MSNPs functionalized with 3-trihydroxysilylpropyl methyl phosphonate that were made using two concentrations of PEI (L=5 mg/ml and H=8 mg/ml)
- Figure 4. Selected area electron diffraction pattern and EADX of AuNP-inserted unmodified MSNPs that were made at two concentrations of PEI (L=5 mg/ml and H=8 mg/ml)
- Figure 5. Selected area electron diffraction pattern and EADX of AuNP-inserted 3-trihydroxysilylpropyl methyl phosphonate-modified MSNPs that were made at two concentrations of PEI (L=5 mg/ml and H=8 mg/ml).
- Figure 6. HR SEM images of AuNP-inserted unmodified MSNPs that were made at two concentrations of PEI (L=5 mg/ml and H=8 mg/ml).
- Figure 7. HR SEM images of AuNP-inserted MSNPs functionalized with 3-trihydroxysilylpropyl methyl phosphonate that were made at two concentrations of PEI (L=5 mg/ml and H=8 mg/ml).
- Figure 8. AuNP-mediated oxidation of o-dianisidine.
- Figure 9. a) Time-dependent absorbance changes at 430 nm in the presence of (A) AuNP-inserted in unmodified MSNP and (B) AuNP-inserted MSNPs that were functionalized with 3-trihydroxysilylpropyl methyl phosphonate. b) Relative peroxidase mimetic activity of trihydroxysilylpropyl methyl phosphonate-modified AuNP-inserted MSNPs, unmodified AuNP-inserted MSNPs, and MSNPs without AuNPs. c) Glucose concentration-response curve for glucose detection using glucose oxidase enzyme and odianisidine in the presence of AuNP-inserted MSNPs. d) Linear calibration plot for glucose analysis.
- Figure 10. a) Visual photographs showing a decrease in color intensity of the oxidized product of o-dianisidine as a function of GSH concentration from 0 μM to 100 μM. b) UV-VIS spectra of the colored reaction product of o-dianisidine as a function of GSH concentrations; 1=0 μM, 2= 10 μM, 3=20 μM, 4= 50 μM and 5= 100 μM. b) GSH-response for glutathione detection based on competitive interaction in the presence of AuNP-inserted MSNPs. c) Linear calibration plot for GSH analysis. d) Reusability of AuNP-inserted MSNPs after repeated cycles of GSH detection.
- Figure 11. Relative catalytic activity for GSH sensing based on competitive binding.
- Figure 12. a) Paclitaxel loading as a function PEI functionalization; the PEI concentrations in MSNP (H) and MSNP (L) were 8 mg/ml and 5 mg/ml respectively. b) Paclitaxel loading as a function of PEI concentration.

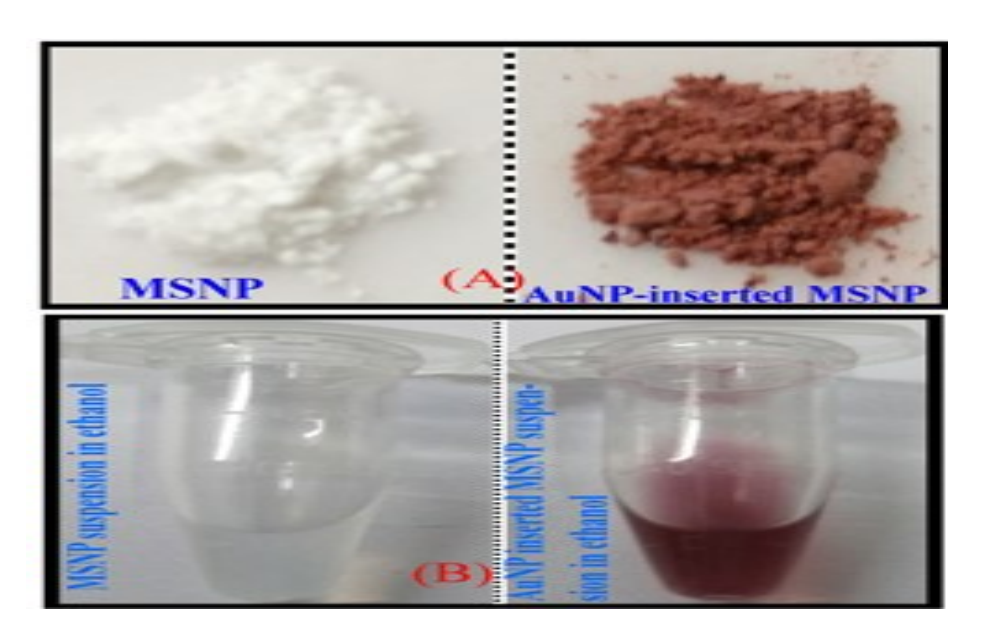


Figure 1.

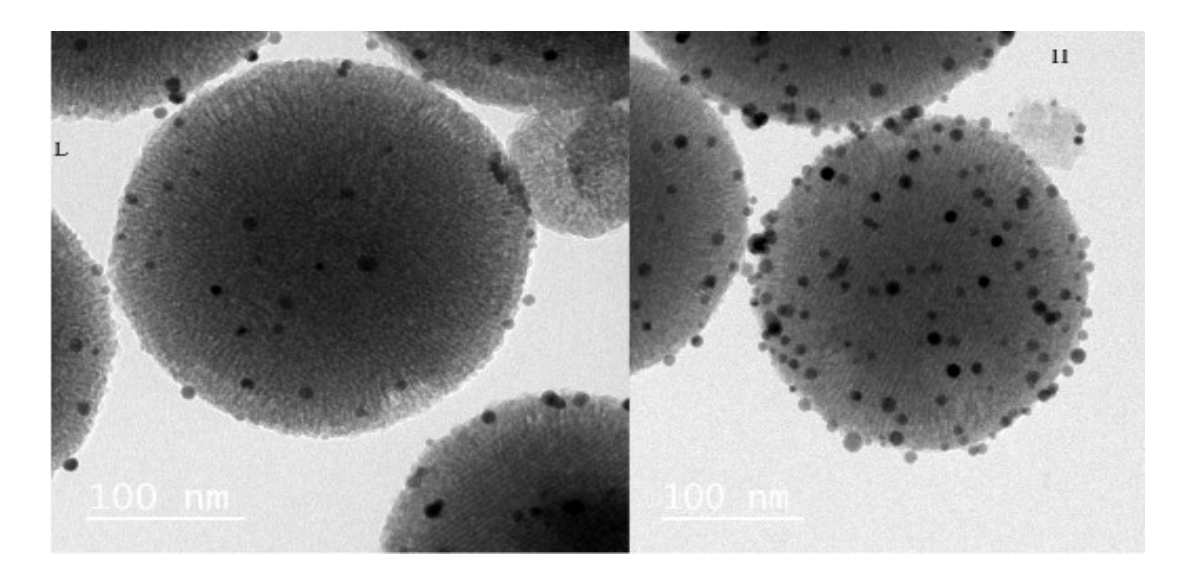


Figure 2.

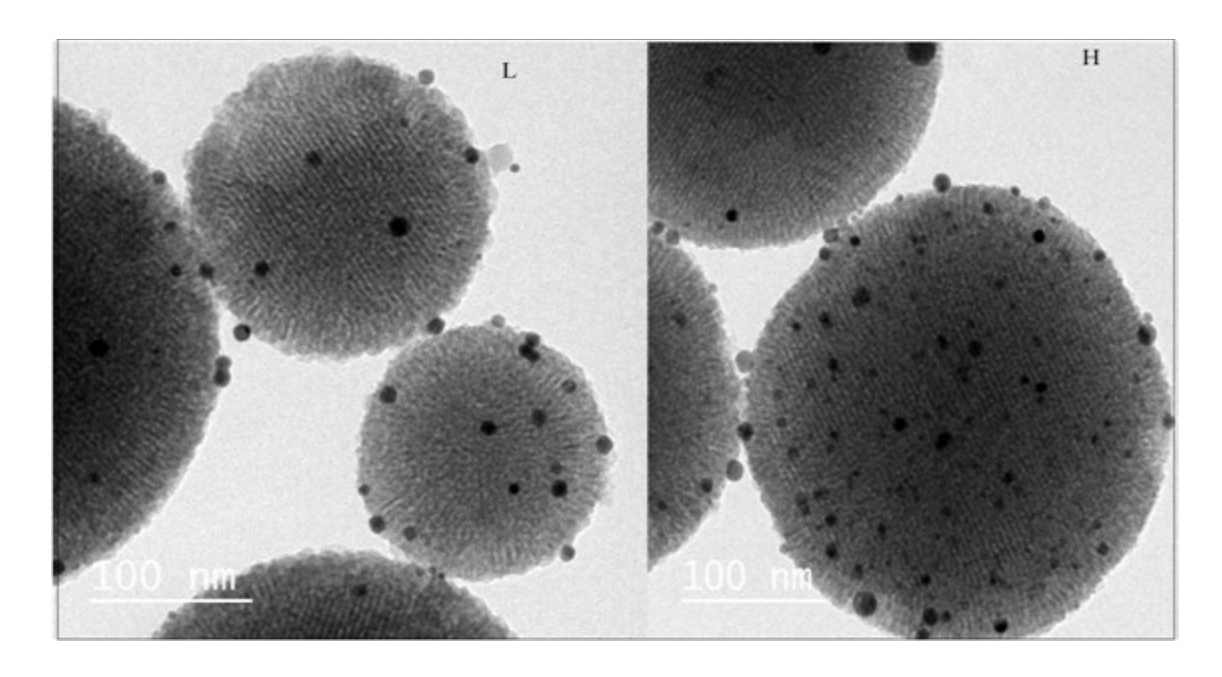


Figure 3.

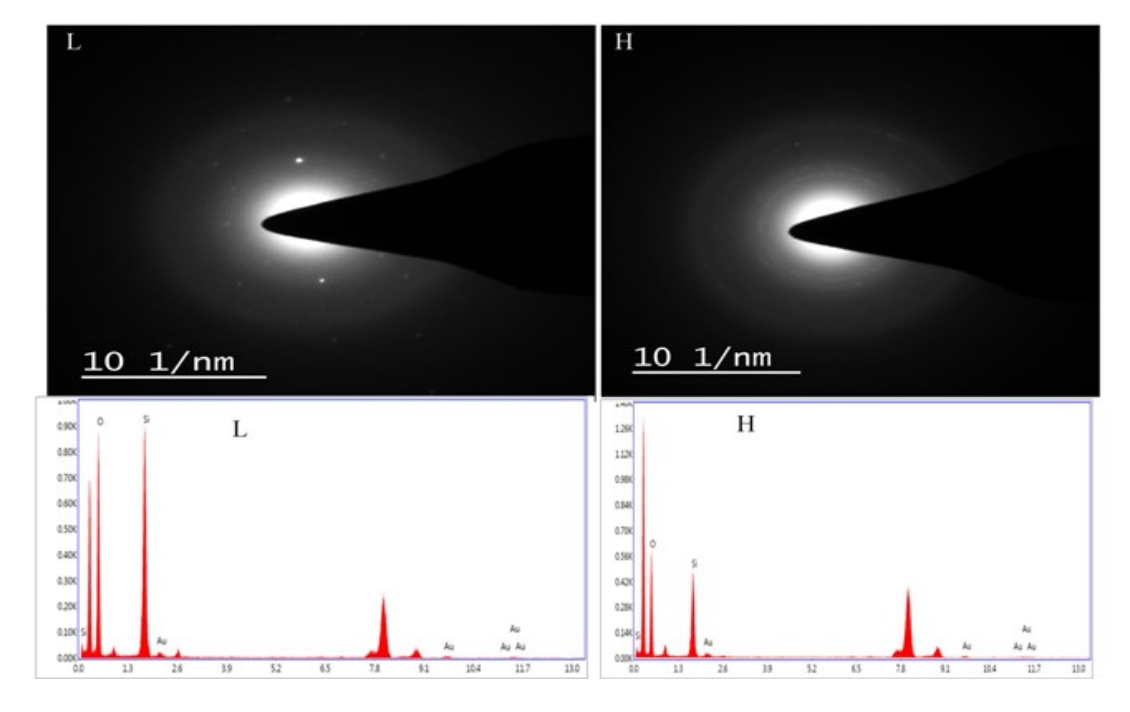


Figure 4.

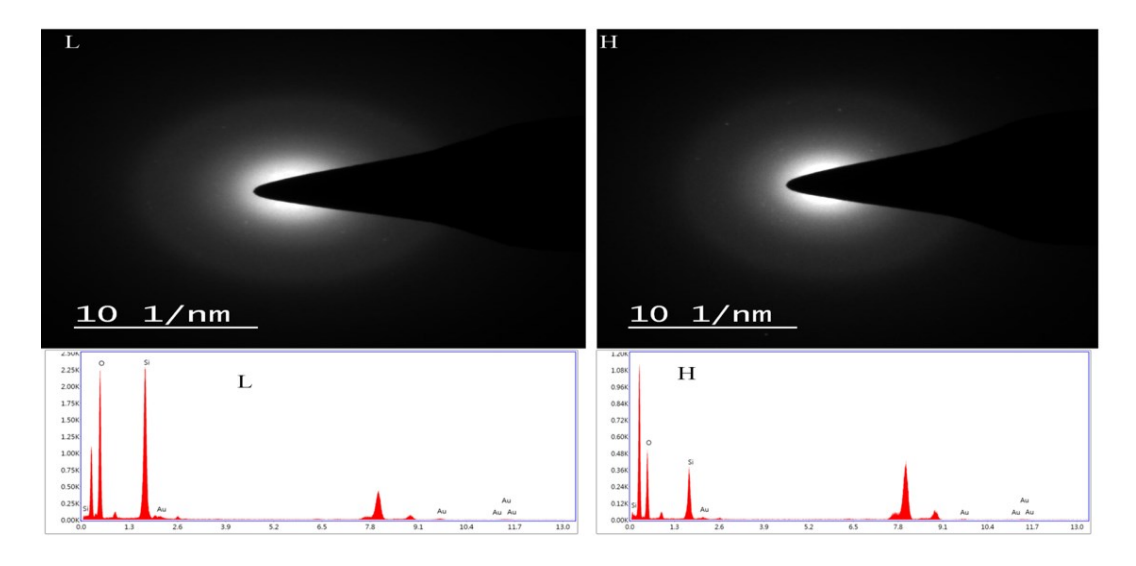


Figure 5.

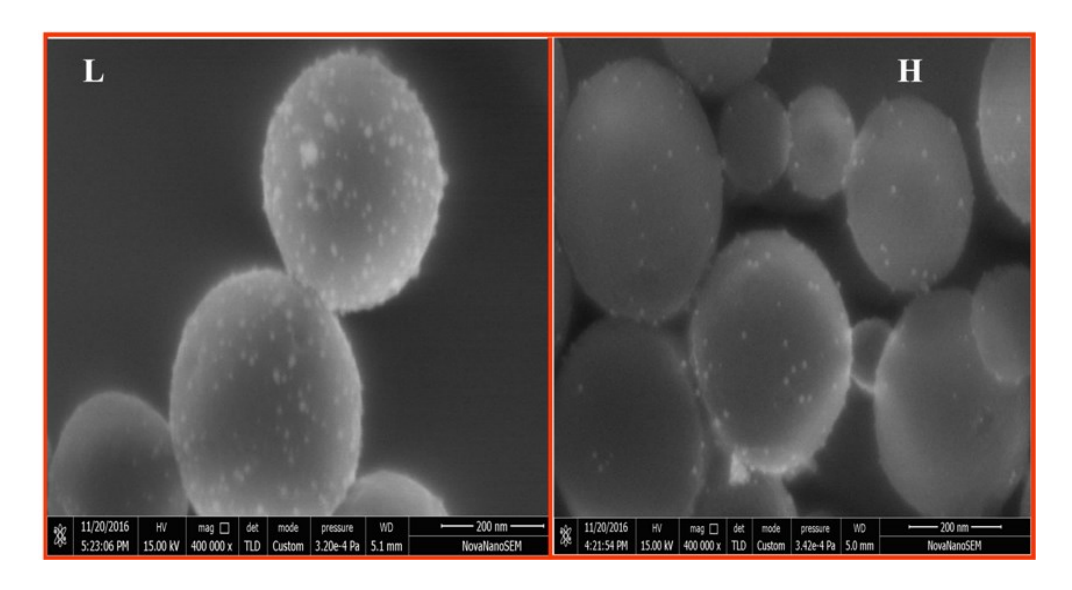


Figure 4.

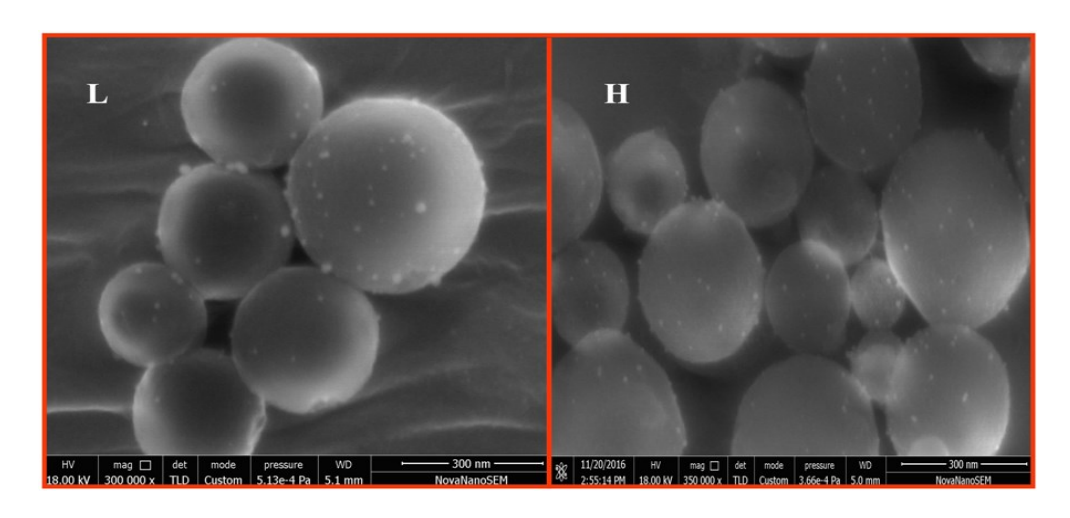


Figure 5.

Figure 8.

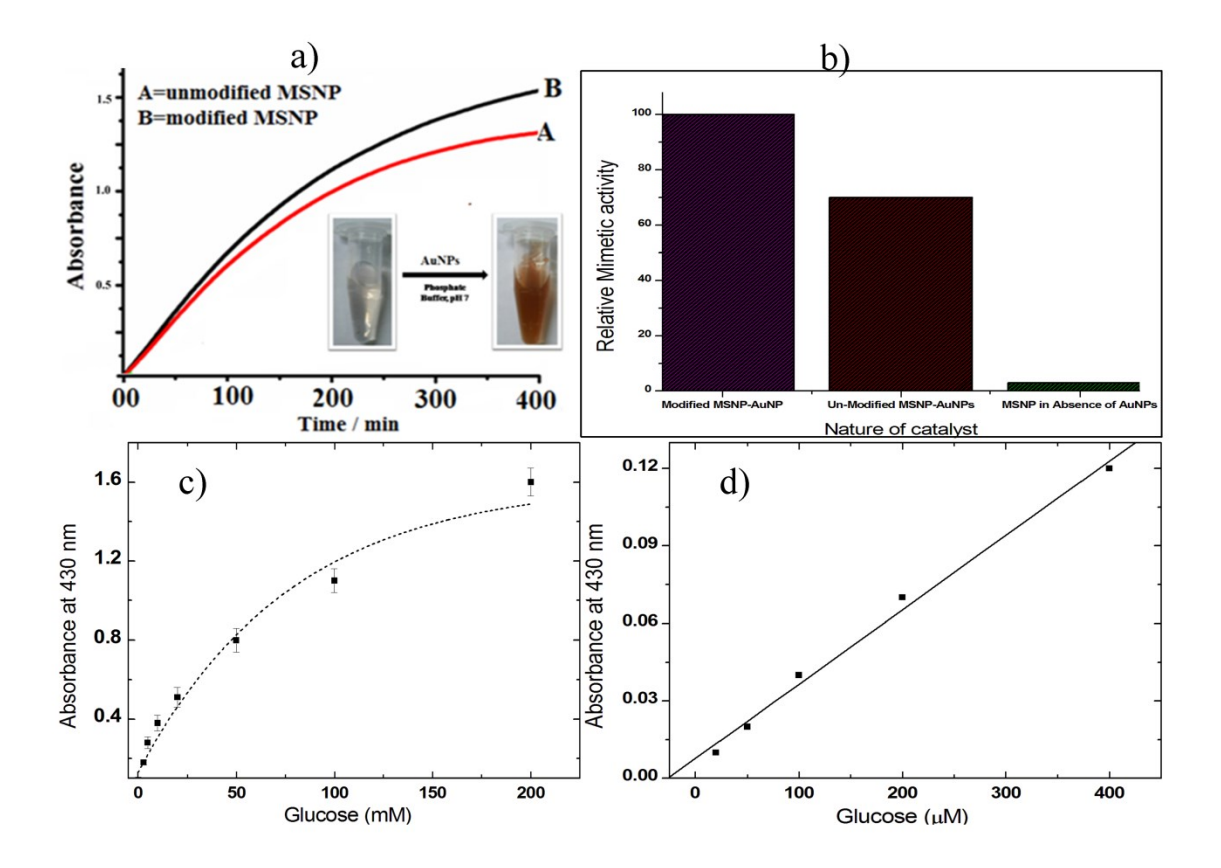


Figure 9.

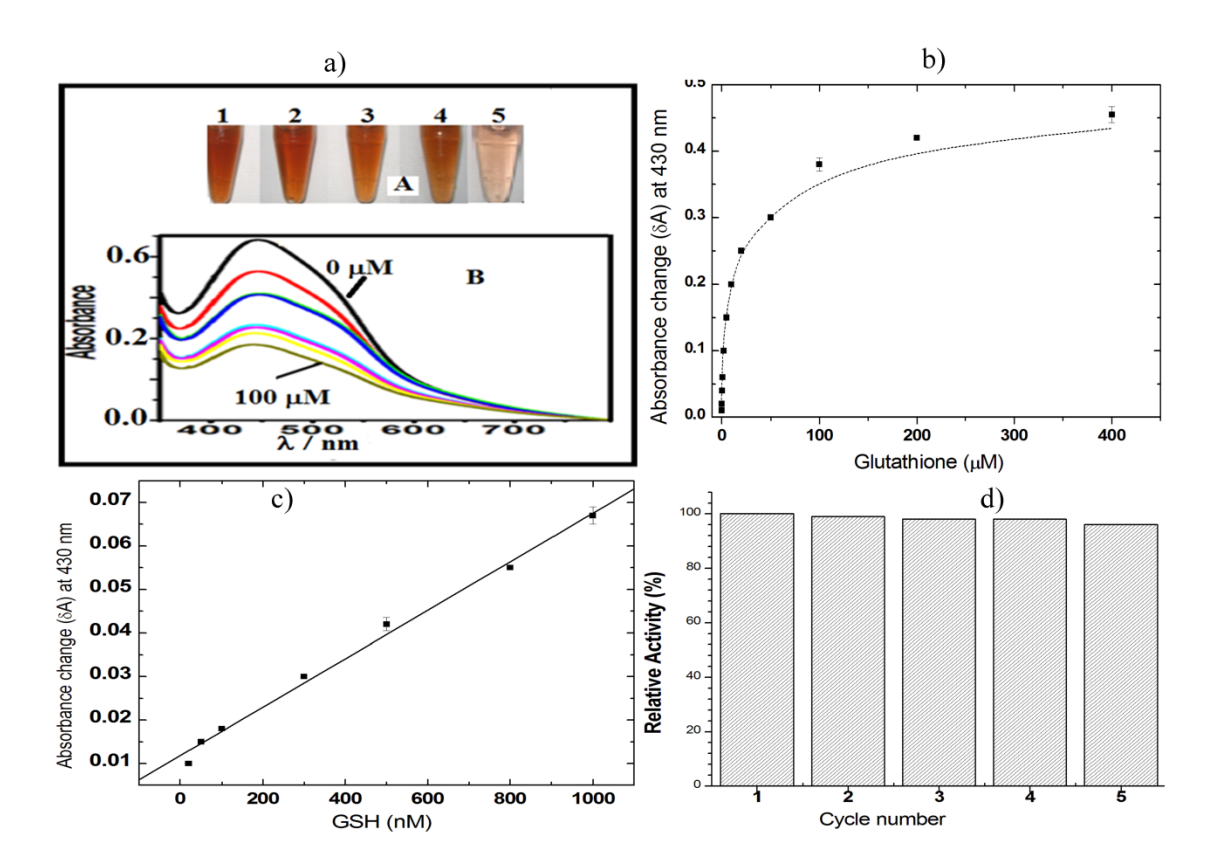


Figure 10.

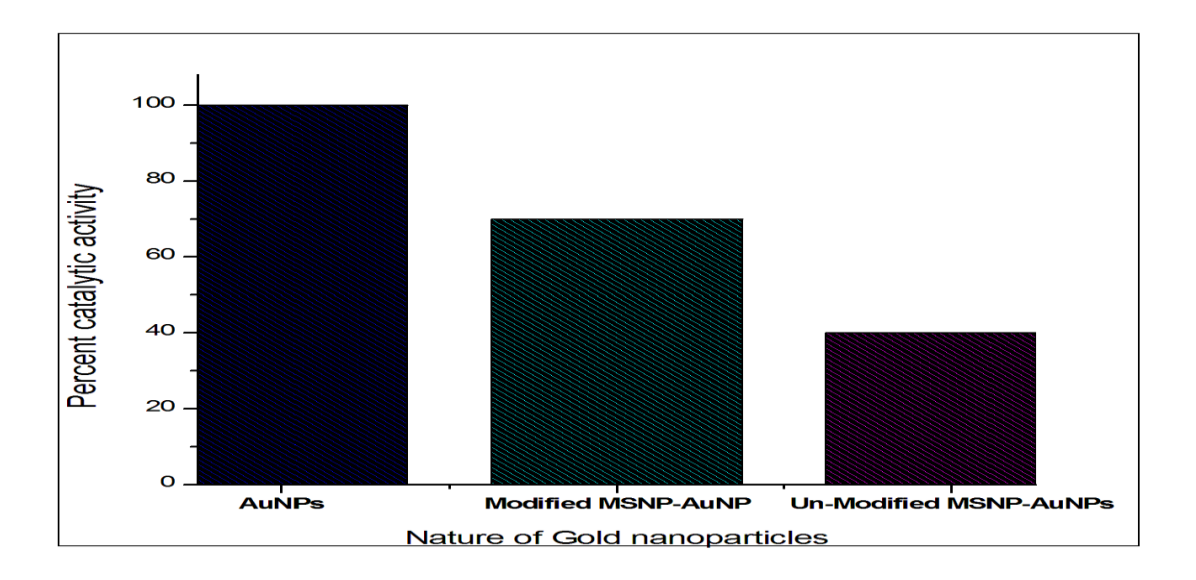


Figure 11.

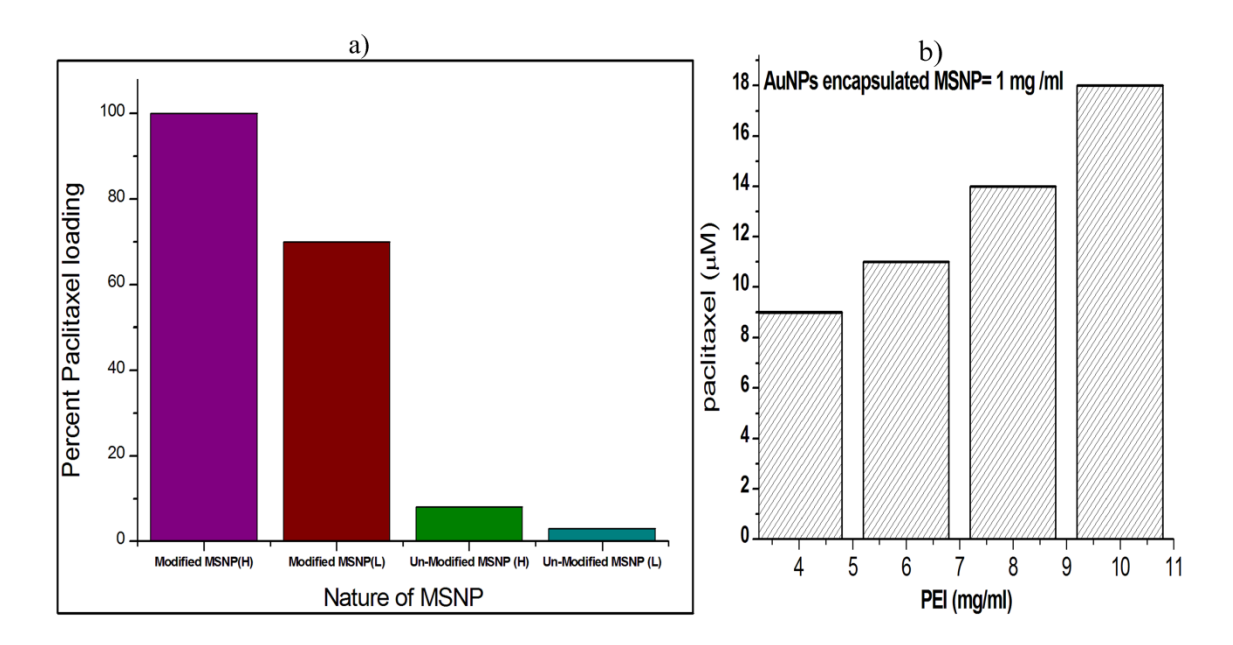


Figure 12.